AD-A031 168 DAVID W TAYLOR NAVAL SHIP RESEARCH AND DEVELOPMENT CE--ETC F/G 20/4
SIMILARITY-LAW ENTRAINMENT METHOD FOR THICK AXISYMMETRIC TURBUL--ETC(U)
DEC 75 P S GRANVILLE

UNCLASSIFIED DTNSRDC-4525 NL

1 OF 1
AD A031168

END

DATE FILMED
11-76

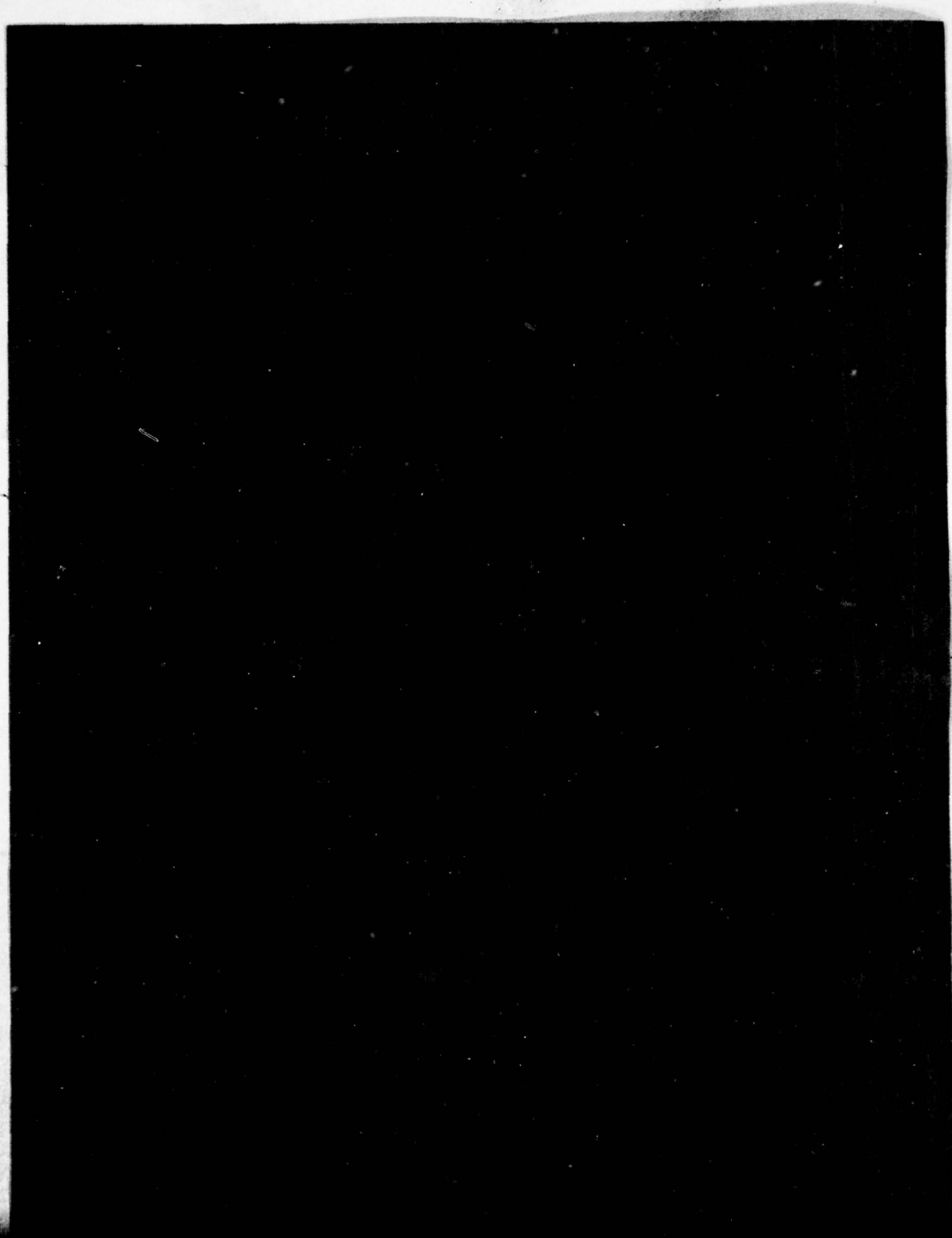

UNCLASSIFIED

SECURITY CLASSIFICATION OF THIS PAGE (When Data Entered)

REPORT DOCUMENTATION PAGE

READ INSTRUCTIONS BEFORE COMPLETING FORM

1. REPORT NUMBER: 4525

2. GOVT ACCESSION NO.

3. RECIPIENT'S CATALOG NUMBER

4. TITLE (and Subtitle): SIMILARITY-LAW ENTRAINMENT METHOD FOR THICK AXISYMMETRIC TURBULENT BOUNDARY LAYERS IN PRESSURE GRADIENTS.

5. TYPE OF REPORT & PERIOD COVERED

6. PERFORMING ORG. REPORT NUMBER

7. AUTHOR(s): Paul S. Granville

8. CONTRACT OR GRANT NUMBER(s)

9. PERFORMING ORGANIZATION NAME AND ADDRESS
David W. Taylor Naval Ship Research and Development Center
Bethesda, Maryland 20084

10. PROGRAM ELEMENT, PROJECT, TASK AREA & WORK UNIT NUMBERS
Project ZR-023-0101
Work Unit 1-1541-002

11. CONTROLLING OFFICE NAME AND ADDRESS: Research and development rept.,

12. REPORT DATE: December 1975

13. NUMBER OF PAGES: 39

14. MONITORING AGENCY NAME & ADDRESS(if different from Controlling Office): DTNSRDC-4525

15. SECURITY CLASS. (of this report): UNCLASSIFIED

15a. DECLASSIFICATION/DOWNGRADING SCHEDULE

16. DISTRIBUTION STATEMENT (of this Report)

37p.

APPROVED FOR PUBLIC RELEASE: DISTRIBUTION UNLIMITED

17. DISTRIBUTION STATEMENT (of the abstract entered in Block 20, if different from Report)

ZR023-01 ZR023-01-01

18. SUPPLEMENTARY NOTES

19. KEY WORDS (Continue on reverse side if necessary and identify by block number)
Thick axisymmetric boundary layer
Turbulent boundary layer
Pressure gradient

20. ABSTRACT (Continue on reverse side if necessary and identify by block number)

Analytical relations have been derived for calculating developing thick, axisymmetric, turbulent boundary layer in a pressure gradient from two simultaneous differential equations: momentum and shape parameter. An entrainment method is used to obtain the shape parameter equation. Both equations incorporate the velocity similarity laws that provide a two-parameter velocity profile general enough to include *any range of Reynolds numbers*. Newly defined "quadratic" shape parameters which arise from the geometry

(Continued on reverse side)

DD FORM 1 JAN 73 1473 EDITION OF 1 NOV 65 IS OBSOLETE
S/N 0102-014-6601

UNCLASSIFIED 387682
SECURITY CLASSIFICATION OF THIS PAGE (When Data Entered)

(Block 20 continued)

of the thick axisymmetric boundary layer are analytically related to the two-dimensional shape parameter by means of these velocity similarity laws.

The variation of momentum loss, boundary-layer thickness, local skin friction, and local velocity profile may be calculated for the axisymmetric turbulent boundary layers on underwater bodies, including the thick boundary layers on the tails. The various formulations are shown to correlate well with available experimental data.

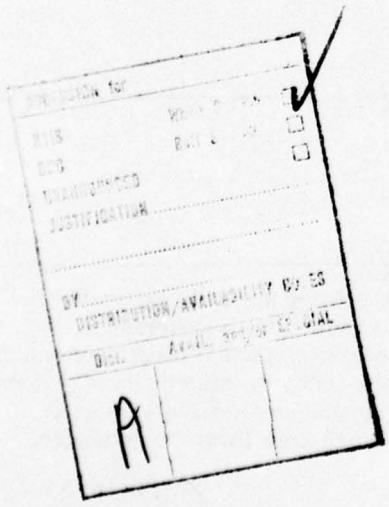

TABLE OF CONTENTS

LIST OF FIGURES

NOTATION

A	Slope of logarithmic velocity law
a_1, a_2, a_3	Constants in Equation (66)
B_1	Law-of-the-wall factor
B_2	Velocity-defect factor
E	Entrainment factor, Equation (21)
G	Rotta-Clauser shape parameter, Equation (50)
$\tilde{G}$	Part of G affected by pressure gradients
ΔG	Part of G affected by low Reynolds number
H	Shape parameter, Equation (30)
H_Δ	"Quadratic" displacement shape parameter, Equation (35)
H_ϕ	"Quadratic" momentum shape parameter, Equation (36)
H_ψ	"Quadratic" entrainment shape parameter, Equation (42)
$\tilde{H}$	Entrainment shape parameter, Equation (41)
I_1	Velocity-defect integral, Equation (46)
I_2	Velocity-defect integral, Equation (48)
J_1	"Quadratic" velocity-defect integral, Equation (47)
J_2	"Quadratic" velocity-defect integral, Equation (49)
L	Length of body
ℓ	Axial distance from nose of body
n	Exponent in power-law velocity profile
p	Pressure
$\hat{p}$	Cross-pressure term
p_δ	Pressure at outer edge of boundary layer
q	Wake-modification function
R_θ	Momentum-thickness Reynolds number
r	Radial distance from axis of body of revolution
r_w	Local radius of body of revolution
r_δ	Value of r at outer edge of boundary layer
s	Streamwise distance
U	Velocity at outer edge of boundary layer

u	Streamwise velocity component
u_τ	Shear velocity
v	Normal velocity component
v_δ	Value of v at outer edge of boundary layer
w	Wake function
x	Relative axial distance = ℓ/L
y	Normal distance from wall
α	Angle between contour tangent and axis
β	Clauser pressure gradient parameter
Δ	"Quadratic" displacement area, Equation (32)
δ	Boundary-layer thickness
δ^*	Two-dimensional displacement thickness, Equation (28)
θ	Two-dimensional momentum thickness, Equation (29)
Λ^*	Displacement area, Equation (7)
ν	Kinematic viscosity of fluid
ρ	Density of fluid
σ	Local skin-friction coefficient
$\tilde{\sigma}$	Turbulent normal stress in y-direction
$\hat{\sigma}$	Normal stress term
σ_t	Turbulent normal stress in s-direction
τ	Shearing stress
τ_w	Wall shearing stress
ϕ	"Quadratic" momentum area, Equation (34)
ψ	Axisymmetric entrainment area, Equation (27)
Ω	Momentum area, Equation (6)

ABSTRACT

Analytical relations have been derived for calculating developing thick, axisymmetric, turbulent boundary layers in a pressure gradient from two simultaneous differential equations: momentum and shape parameter. An entrainment method is used to obtain the shape parameter equation. Both equations incorporate the velocity similarity laws that provide a two-parameter velocity profile general enough to include *any range of Reynolds numbers.* Newly defined "quadratic" shape parameters which arise from the geometry of the thick axisymmetric boundary layer are analytically related to the two-dimensional shape parameter by means of these velocity similarity laws.

The variation of momentum loss, boundary-layer thickness, local skin friction, and local velocity profile may be calculated for the axisymmetric turbulent boundary layers on underwater bodies, including the thick boundary layers on the tails. The various formulations are shown to correlate well with available experimental data.

ADMINISTRATIVE INFORMATION

The work described in this report was authorized and funded by the Independent Research Program of the David W. Taylor Naval Ship Research and Development Center under Project ZR-023-0101, Work Unit 1-1541-002.

INTRODUCTION

Accurate prediction of the viscous drag of bodies of revolution and the associated boundary-layer velocity profiles requires solving equations for the thick, axisymmetric, boundary layer on the tail. At the high Reynolds numbers of interest, the analysis involves the usual difficulties encountered with a turbulent boundary layer in a pressure gradient now accentuated by the boundary layer being thick relative to the body radius.

There are existing methods, having varying degrees of merit, for analyzing the thick, axisymmetric, turbulent boundary layer in a pressure gradient. Nelson[1] derived an energy integral equation and used the similarity laws for the velocity profile. The Coles wake function is fitted by an awkward analytical relation which leads to complicated expressions for the required boundary-layer parameters. The axisymmetric energy dissipation factor which is an essential element in the solution is not separately evaluated but, instead, is

[1] Nelson, D.M., "A Turbulent Boundary-Layer Calculation Method, Based on the Law of the Wall and the Law of the Wake," U.S. Naval Ordnance Test Station (China Lake, Calif.), NavWeps Report 8510 (NOTS TP 3493) (Nov 1964). A complete listing of references is given on page 32.

mistakenly linked back to the equation of motion. The result is that the energy equation is not independent of the momentum equation which is a fundamental error. To correct this, Nelson[2] later empirically evaluated the dissipation integral from two-dimensional test data whose application to axisymmetric conditions has not been established.

Cebeci and Smith[3] use a direct numerical approach in solving the partial differential equations of motion for the boundary layer by the method of finite differences. The unknown turbulent shear stress is modeled for the most part by an eddy viscosity relation previously obtained by Clauser for two-dimensional equilibrium pressure gradients. The eddy viscosity, originally related to the two-dimensional displacement thickness, is extended by Cebeci and Smith to what is essentially a thin axisymmetric displacement thickness. At the after end of a body of revolution where the radius of the body becomes zero, the eddy viscosity so defined becomes infinite and hence invalid.

Patel[4,5] developed a one-parameter entrainment method for thick axisymmetric boundary layers by extending the Head one-parameter entrainment method for two-dimensional boundary layers. In the entrainment equation derived by physical argument for thick, axisymmetric boundary layers, Patel has assumed that the radius of the body is the length scale required to balance the equation dimensionally. On the contrary, an analytical derivation later in this paper shows that the proper length factor is the radial distance to the outside of the boundary layer, which is equal to the radius of the body plus the boundary layer thickness slightly modified by the slope of the body. Since the radius of the body becomes zero at the very end of the body, the Patel analysis shows no entrainment, unlike the more fundamental analysis in this paper. Part of the analysis of the thick, axisymmetric boundary layer involves additional integrations of the velocity profile with respect to the square of the transverse distance which may be termed "quadratic" integration. For these, Patel uses approximate simple power-law velocity profiles.

---

[2]Nelson, D.M., "Turbulent Boundary-Layer Calculations, Using a Law of the Wall-Law of the Wake Method," U.S. Naval Ordnance Test Station (China Lake, Calif.), NOTS TP 4083 (Jun 1966).

[3]Cebeci, T. and A.M.O. Smith, "A Finite-Difference Method for Calculating Compressible Laminar and Turbulent Boundary Layers," Journal of Basic Engineering, Transactions of the American Society of Mechanical Engineers, Vol. 92, Series D, No. 3, pp. 523-535 (Sep 1970).

[4]Patel, V.C., "On the Equations of a Thick Axisymmetric Turbulent Boundary Layer," Iowa Institute of Hydraulic Research Report 143 (Jan 1973).

[5]Patel, V.C., "A Simple Integral Method for the Calculation of Thick Axisymmetric Turbulent Boundary Layers," Aeronautical Quarterly, Vol. 25, part 1, pp. 47-58 (Feb 1974).

Günther[6] presents a complicated energy method that will not be discussed herein. White et al.[7] extend to thick, axisymmetric, turbulent boundary layers a procedure used previously for two-dimensional boundary layers which provides an ordinary differential equation for the streamwise distribution of local skin friction in lieu of the usual momentum equation. To obtain this equation, a constant shearing stress and the inner velocity similarity law are assumed to hold across the entire boundary layer. These two assumptions are quite contrary to experimental evidence.

In this paper the integral approach is followed wherein the axisymmetric boundary-layer equations are symbolically integrated, and an appropriate velocity profile is inserted to obtain a numerical solution. Integration of the streamwise equation of motion with the assistance of the equation of continuity gives the well-known momentum equation. The integration of the equation of continuity gives a new entrainment equation. The result is an entrainment factor multiplied by the radial distance to the outer edge of the boundary layer instead of the radius of the body as used by Patel.[5]

The required velocity profile is supplied by the well-established velocity similarity laws for turbulent boundary layers in pressure gradients which comprise an essentially two-parameter velocity profile system. A newly modified expression for the law of the wake is employed for the analytical description of the similarity laws. The local skin friction is supplied by the similarity laws.

The axisymmetric boundary layer developing downstream on the tail of a body of revolution becomes thicker from viscous losses and adverse pressure gradients – significantly thicker than the body radius, which is approaching zero at the tail end of the body. What happens is that geometrically the annular boundary layer in the transverse plane ends as a disk at the tail end. The thick boundary layer fills a thick annular space which leads to quadratic terms in integrations of the velocity profile which do not exist in two-dimensional flow or are negligible for thin, axisymmetric boundary layers. Newly defined quadratic shape parameters are accordingly introduced and are evaluated from the similarity laws.

For simplicity of solution, all parameters are expressed in terms of the usual two-dimensional momentum thickness and shape parameter.

It is shown that the momentum and entrainment equations which are ordinary differential equations may be readily solved in a stepwise fashion suitable for easily formulated

---

[6]Günther, W., "Ein mehrparametrisches Rechenfahren für turbulente, inkompressible Grenzschichten an umströmten Rotationskörpern," Fortschritt-Berichte der VDI Zeitschriften, Series 7, No. 34 (Oct 1973).

[7]White, F.M. et al., "Analysis of Turbulent Skin Friction in Thick Axisymmetric Boundary Layers," American Institute of Aeronautics and Astronautics Journal, Vol. 11, No. 6, pp. 821-835 (Jun 1973).

computer programs. Finally, the new formulas for the quadratic shape parameters are shown to agree with available experimental data.

AXISYMMETRIC TURBULENT BOUNDARY LAYERS

COORDINATE SYSTEM

The coordinate system for the boundary layer on a body of revolution is obtained from two families of surfaces. One family is given by surfaces parallel to the given body of revolution displaced by a normal distance y. The other family is orthogonal to the family of parallel bodies of revolution and is separated by contour distance s. The coordinate system then is s along a body meridian with s = 0 at the nose, and y is normal to the body surface with y = 0 on the body. For axisymmetric flow only two coordinates are required.

At any point (s, y) there is a radial distance to the axis of the body of revolution r so that as seen in Figure 1

$$r = r_w + y \cos \alpha \tag{1}$$

where r_w is the radial distance to the body surface, and α is the angle between the contour tangent and the axis.

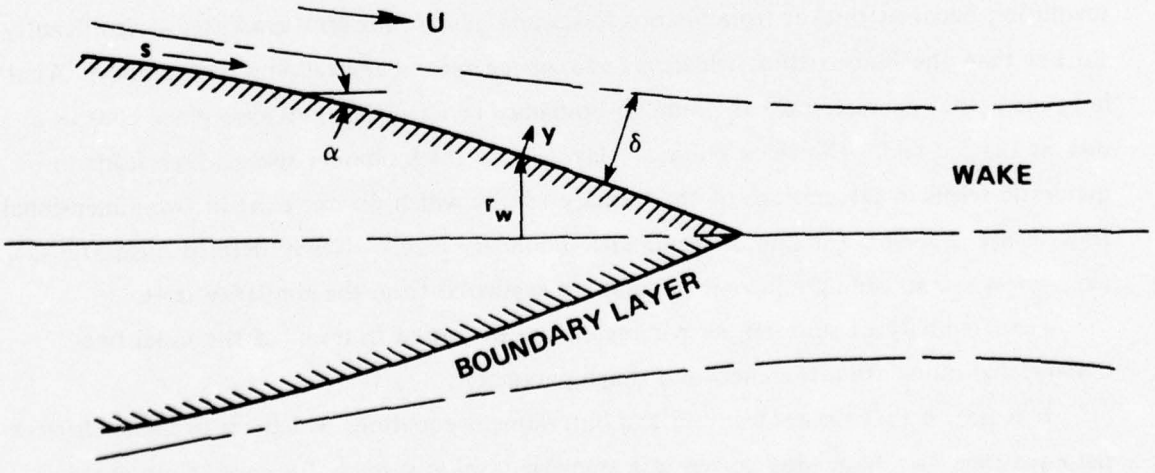

Figure 1 – Thick Axisymmetric Boundary Layer

EQUATIONS OF MOTION

For turbulent flow the Reynolds equations, which are the averaged Navier-Stokes equations, are applied to the boundary-layer flow. For the body-of-revolution coordinate system the Reynolds equations of motion[8] for incompressible flow, neglecting longitudinal curvature, are in the s-direction

$$u \frac{\partial u}{\partial s} + v \frac{\partial u}{\partial y} = - \frac{1}{\rho} \frac{\partial p}{\partial s} + \frac{1}{\rho r} \frac{\partial}{\partial y} (r\tau) - \frac{1}{\rho r} \frac{\partial}{\partial s} (r\sigma_t) \tag{2}$$

and in the y-direction

$$u \frac{\partial v}{\partial y} + v \frac{\partial v}{\partial y} = - \frac{1}{\rho} \frac{\partial p}{\partial y} + \frac{1}{\rho r} \frac{\partial}{\partial s} (r\tau) - \frac{1}{\rho r} \frac{\partial}{\partial y} (r\tilde{\sigma}) \tag{3}$$

and the equation of continuity is

$$\frac{\partial (ru)}{\partial s} + \frac{\partial (rv)}{\partial y} = 0 \tag{4}$$

where u = velocity in s-direction

v = velocity in y-direction

τ = shearing stress, including that due to turbulence

σ_t = turbulent normal stress in s-direction

$\tilde{\sigma}$ = turbulent normal stress in y-direction

p = pressure

ρ = density of fluid

MOMENTUM EQUATION

The momentum equation is obtained by integrating the s-equation of motion Equation (2) from $y = 0$ to $y = \delta$ and incorporating the equation of continuity Equation (4).

The result is the momentum equation for thick axisymmetric boundary layers

$$\frac{d\Omega}{ds} + \frac{(\Lambda^* + 2\Omega)}{U} \frac{dU}{ds} = r_w \frac{\tau_w}{\rho U^2} - \frac{1}{\rho U^2} \frac{d}{ds} \int_o^\delta (p_\delta - p)\, r\, dy + \frac{1}{\rho U^2} \frac{d}{ds} \int_o^\delta \sigma_t r\, dy \tag{5}$$

[8] Granville, P.S., "The Calculation of the Viscous Drag of Bodies of Revolution," David Taylor Model Basin Report 849 (Jul 1953).

where Ω = momentum area

$$\Omega \equiv \int_0^{\delta} \left(1 - \frac{u}{U}\right) \frac{u}{U} r \, dy \tag{6}$$

Λ^* = displacement area

$$\Lambda^* \equiv \int_0^{\delta} \left(1 - \frac{u}{U}\right) r \, dy \tag{7}$$

τ_w = wall shearing stress

p_δ = pressure at outer edge of boundary layer

U = velocity at outer edge of boundary layer

It is to be noted that no boundary-layer simplifications have been made other than neglect of longitudinal curvature. The only assumption is that a boundary layer of thickness δ exists wherein all viscous effects are concentrated.

ENTRAINMENT EQUATION

Besides the momentum equation Equation (5), an additional "integral" equation is needed to calculate development of the boundary layer along the body. The entrainment method introduced by Head[9] has proved effective in this regard for two-dimensional flows in pressure gradients.

The entrainment method will now be developed for the thick axisymmetric boundary layer. The procedure to be followed is to integrate the equation of continuity across the boundary layer and then to evaluate the ensuing entrainment velocity in terms of conditions at the outer edge of the boundary layer. The equation of continuity Equation (4) is integrated from $y = 0$ to $y = \delta$

$$\int_0^{\delta[s]} \frac{\partial(ru)}{\partial s} \, dy + \int_0^{\delta[s]} \frac{\partial(rv)}{\partial y} \, dy = 0 \tag{8}$$

to give by means of the Leibnitz formula and $v = 0$ at $y = 0$

[9] Head, M.R., "Entrainment in the Turbulent Boundary Layer," Aeronautical Research Council (British), R & M 3152 (Sep 1958).

$$\frac{d}{ds}\int_o^\delta ur\,dy - r_\delta U\frac{d\delta}{ds} + r_\delta v_\delta = 0 \tag{9}$$

where the subscript δ refers to conditions at $y = \delta$. Now $v_\delta = v$ at $y = \delta$ is defined to be the entrainment velocity, and from Equation (1)

$$r_\delta = r_w + \delta\cos\alpha \tag{10}$$

To determine the entrainment velocity v_δ, the equation of motion Equation (2) is evaluated at the outer edge of the boundary layer, $y = \delta$

$$r_\delta U\left(\frac{\partial u}{\partial s}\right)_\delta + r_\delta v_\delta\left(\frac{\partial u}{\partial y}\right)_\delta = -\frac{r_\delta}{\rho}\left(\frac{\partial p}{\partial s}\right)_\delta + \frac{1}{\rho}\left(\frac{\partial r\tau}{\partial y}\right)_\delta - \frac{1}{\rho}\left(\frac{\partial r\sigma_t}{\partial s}\right)_\delta \tag{11}$$

Various terms of this expression are to be examined. In general along a streamline

$$\frac{du}{ds} = \frac{\partial u}{\partial s} + \frac{\partial u}{\partial y}\frac{dy}{ds} \tag{12}$$

and then at $y = \delta$

$$\left(\frac{\partial u}{\partial s}\right)_\delta = \frac{dU}{ds} - \left(\frac{\partial u}{\partial y}\right)_\delta\frac{d\delta}{ds} \tag{13}$$

Likewise

$$\left(\frac{\partial r\sigma_t}{\partial s}\right)_\delta = \left(\frac{dr\sigma_t}{ds}\right)_\delta - \left(\frac{\partial r\sigma_t}{\partial y}\right)_\delta\frac{d\delta}{ds} \tag{14}$$

and

$$\left(\frac{\partial p}{\partial s}\right)_\delta = -\rho U\frac{dU}{ds} - \left(\frac{\partial p}{\partial y}\right)_\delta\frac{d\delta}{ds} \tag{15}$$

where the Bernoulli theorem has been applied at the outer edge of the boundary layer

$$\left(\frac{dp}{ds}\right)_\delta + \rho U\frac{dU}{ds} = 0 \tag{16}$$

Furthermore with $\tau = 0$, and $\sigma_t = 0$ at $y = \delta$

$$\left(\frac{\partial r\tau}{\partial y}\right)_\delta = r_\delta\left(\frac{\partial\tau}{\partial y}\right)_\delta, \quad \left(\frac{dr\sigma_t}{ds}\right)_\delta = 0 \tag{17}$$

and

$$\left(\frac{\partial r\sigma_t}{\partial y}\right)_\delta = r_\delta\left(\frac{\partial \sigma_t}{\partial y}\right)_\delta \tag{18}$$

With the foregoing the entrainment velocity given in Equation (11) becomes

$$v_\delta = U\frac{d\delta}{ds} + \frac{1}{\rho}\left(\frac{\partial \tau}{\partial u}\right)_\delta + \frac{1}{\rho}\left[\frac{\partial(p+\sigma_t)}{\partial u}\right]_\delta \frac{d\delta}{ds} \tag{19}$$

Then the entrainment equation Equation (9) becomes in turn

$$\frac{d}{ds}\int_o^\delta ur\,dy = -\frac{r_\delta}{\rho}\left\{\left(\frac{\partial \tau}{\partial u}\right)_\delta + \left[\frac{\partial(p+\sigma_t)}{\partial u}\right]_\delta \frac{d\delta}{ds}\right\} \tag{20}$$

The nondimensional entrainment factor E is now defined as

$$E = -\frac{1}{\rho U}\left\{\left(\frac{\partial \tau}{\partial u}\right)_\delta + \left[\frac{\partial(p+\sigma_t)}{\partial u}\right]_\delta \frac{d\delta}{ds}\right\} \tag{21}$$

This is an expanded definition of E to include the pressure p variation and normal stress σ_t variation in the y direction. Finally the entrainment equation for the thick axisymmetric boundary layer is

$$\frac{d}{ds}\int_o^\delta ur\,dy = r_\delta U E \tag{22}$$

The entrainment equation Equation (22) is more fundamentally based than that introduced by Patel[5] for the thick axisymmetric boundary layer, namely,

$$\frac{d}{ds}\int_o^\delta ur\,dy = r_w U E \tag{23}$$

where r_w is used instead of r_δ. Patel adopted r_w as a convenient nondimensionalizing factor in an analysis based mostly on physical argument.

For the thin axisymmetric boundary layer $\delta << r_w$, the entrainment equation reduces to

$$\frac{d}{ds}\left(r_w\int_o^\delta u\,dy\right) = r_w U E \tag{24}$$

which is the same as the equation derived by Shanebrook and Sumner.[10]

For constant r_w the entrainment equation reduces finally to

$$\frac{d}{ds}\int_o^\delta u\,dy = U\,E \tag{25}$$

This is the same as the **Head[9] two-dimensional equation.**

For the thick axisymmetric boundary layer the entrainment equation may also be expressed as

$$\frac{d\psi}{ds} = r_\delta\,E - \frac{\psi}{U}\frac{dU}{ds} \tag{26}$$

where

$$\psi = \int_o^\delta \frac{u}{U}\,r\,dy \tag{27}$$

is a newly defined axisymmetric entrainment area.

INTEGRAL VELOCITY FACTORS FOR AXISYMMETRIC FLOW

In analysis of two-dimensional boundary layers, the displacement thickness δ^*, the momentum thickness θ, and their ratio H, the shape parameter, are defined as

$$\delta^* \equiv \int_o^\delta \left(1 - \frac{u}{U}\right) dy \tag{28}$$

$$\theta \equiv \int_o^\delta \left(1 - \frac{u}{U}\right)\frac{u}{U}\,dy \tag{29}$$

and

$$H \equiv \delta^*/\theta \tag{30}$$

For axisymmetric boundary layers, the displacement thickness δ^* becomes the displacement area Λ^*, which has been previously defined as

$$\Lambda^* \equiv \int_o^\delta \left(1 - \frac{u}{U}\right) r\,dy \tag{7}$$

[10]Shanebrook, J.R. and W. J. Sumner, "Entrainment Theory for Axisymmetric, Turbulent, Incompressible Boundary Layers," Journal of Hydronautics, Vol. 4, No. 4, pp. 159-160 (Oct 1970).

and the momentum thickness θ becomes the momentum area Ω which has been previously defined as

$$\Omega \equiv \int_o^\delta \left(1 - \frac{u}{U}\right) \frac{u}{U} \, r \, dy \tag{6}$$

Further analysis yields quadratic factors such as Δ and ϕ. From Equation (1)

$$\Lambda^* = r_w \, \delta^* + \Delta \cos \alpha \tag{31}$$

where

$$\Delta \equiv \int_o^\delta \left(1 - \frac{u}{U}\right) y \, dy \tag{32}$$

Likewise

$$\Omega = r_w \, \theta + \phi \cos \alpha \tag{33}$$

where

$$\phi \equiv \int_o^\delta \left(1 - \frac{u}{U}\right) \frac{u}{U} \, y \, dy \tag{34}$$

Additional quadratic shape factors may now be defined such as H_Δ and H_ϕ,

$$H_\Delta \equiv \frac{\Delta}{\theta^2} \tag{35}$$

and

$$H_\phi \equiv \frac{\phi}{\theta^2} \tag{36}$$

Consequently the displacement area and the momentum area may be related to momentum thickness θ by

$$\Lambda^* = r_w \, H\theta + H_\Delta \theta^2 \cos \alpha \tag{37}$$

and

$$\Omega = r_w \, \theta + H_\phi \theta^2 \cos \alpha \tag{38}$$

It follows from the definitions given in Equations (1), (7), and (27) that

$$\psi = r_w \, (\delta - \delta^*) + \left(\frac{\delta^2}{2} - \Delta\right) \cos \alpha \tag{39}$$

or

$$\psi = r_w \tilde{H}\theta + H_\psi \theta^2 \cos\alpha \tag{40}$$

where $\tilde{H}$ is the two-dimensional entrainment shape parameter defined by

$$\tilde{H} \equiv \frac{\delta - \delta^*}{\theta} = \frac{\delta}{\theta} - H \tag{41}$$

and H_ψ is a quadratic entrainment shape parameter newly defined

$$H_\psi \equiv \frac{\frac{\delta^2}{2} - \Delta}{\theta^2} = \frac{1}{2}\left(\frac{\delta}{\theta}\right)^2 - \frac{\Delta}{\theta^2} \tag{42}$$

Consequently

$$H_\psi = \frac{1}{2}\left(\frac{\delta}{\theta}\right)^2 - H_\Delta = \frac{1}{2}(\tilde{H} + H)^2 - H_\Delta \tag{43}$$

SIMILARITY LAWS AND ASSOCIATED INTEGRALS

From a study of experimental data Nelson[1] has concluded that the similarity laws of the turbulent velocity profile apply to the thick, axisymmetric boundary layer in a pressure gradient as well as to the more thoroughly studied two-dimensional boundary layer.

The two velocity similarity laws[11] implicitly provide a two-parameter system, an inner law

$$\frac{u}{u_\tau} = f\left[\frac{u_\tau y}{\nu}\right] \qquad 0 \leq y \leq y_1 \tag{44}$$

and an outer law

$$\frac{U - u}{u_\tau} = f\left[\frac{y}{\delta}\right] \qquad y_2 < y_1 \leq y \leq \delta \tag{45}$$

where $u_\tau = \sqrt{\tau_w/\rho}$, the shear velocity.

The inner law as stated herein applies only to smooth surfaces. For rough surfaces and for drag-reducing polymer solutions, there are additional dimensionless ratios. The outer law, however, applies unchanged to rough surfaces and to drag-reducing polymer solutions. The two similarity laws overlap across the boundary layer, which leads to logarithmic relations.[11]

[11] Granville, P.S., "Similarity-Law Entrainment Method for Turbulent Boundary Layers in Pressure Gradients," DTNSRDC Report 4657 (Dec 1975).

Various new integral relations based on the outer-law form are required in the analysis to come. The usual two-dimensional relation

$$I_1 \equiv \int_0^1 \left(\frac{U - u}{u_\tau}\right) d\left(\frac{y}{\delta}\right) \tag{46}$$

is now extended to axisymmetric flow so that

$$J_1 \equiv \int_0^1 \left(\frac{U - u}{u_\tau}\right)\left(\frac{y}{\delta}\right) d\left(\frac{y}{\delta}\right) \tag{47}$$

Also the usual two-dimensional relation

$$I_2 \equiv \int_0^1 \left(\frac{U - u}{u_\tau}\right)^2 d\left(\frac{y}{\delta}\right) \tag{48}$$

becomes now

$$J_2 \equiv \int_0^1 \left(\frac{U - u}{u_\tau}\right)^2 \left(\frac{y}{\delta}\right) d\left(\frac{y}{\delta}\right) \tag{49}$$

In two-dimensional flow, the Rotta-Clauser shape parameter is defined as

$$G \equiv \frac{I_2}{I_1} = \sigma\left(\frac{H - 1}{H}\right) \tag{50}$$

where $\sigma = U/u_\tau$.

The outer law may be expressed logarithmically[12] as

$$\frac{U - u}{u_\tau} = - A \ln \frac{y}{\delta} + B_2 \left(1 - \frac{w}{2}\right) - A q \tag{51}$$

where $\frac{w}{2}\left[\frac{y}{\delta}\right]$ is the Coles wake function, and $q\left[\frac{y}{\delta}\right]$, the wake-modification function, is added to make $\frac{\partial u}{\partial y} = 0$ at $y = \delta$. A is a constant while B_2, the velocity-defect factor, is a function of s in arbitrary pressure gradients; $\frac{w}{2}$ is given by Moses as

$$\frac{w}{2} = 3\left(\frac{y}{\delta}\right)^2 - 2\left(\frac{y}{\delta}\right)^3 \tag{52}$$

[12] Granville, P.S., "A Modified Velocity Similarity Law for Turbulent Shear Flows," NSRDC Report 4639 (May 1975).

while q is given by Granville as

$$q = \left(\frac{y}{\delta}\right)^2 - \left(\frac{y}{\delta}\right)^3 \tag{53}$$

If the outer law is assumed to hold up to wall, $0 \leqslant y \leqslant \delta$, which is an excellent approximation at high Reynolds numbers, the integral parameters become

$$I_1 = \frac{11}{12} A + \frac{B_2}{2} \tag{54}$$

$$I_2 = \frac{4819}{2520} A^2 + \frac{213}{140} A B_2 + \frac{13}{35} B_2^2 \tag{55}$$

$$J_1 = \frac{1}{5} A + \frac{3}{20} B_2 \tag{56}$$

and

$$J_2 = \frac{443}{2100} A^2 + \frac{359}{1400} A B_2 + \frac{3}{35} B_2^2 \tag{57}$$

where A is the reciprocal of the von Kármán constant and B_2 is the velocity-defect factor. For nonequilibrium pressure gradients, $B_2 = f[s]$.

LOCAL SKIN FRICTION

For the solution of boundary-layer equations such as the momentum equation Equation (5), a most essential ingredient is relating the coefficient of wall shear stress or local skin friction $\frac{\tau_w}{\rho U^2} = \frac{1}{\sigma^2}$ to the local Reynolds number $R_\theta = \frac{U\theta}{\nu}$ and local shape parameter H. As shown in detail in Reference 11, for two-dimensional boundary layers, this is derived from overlapping the inner and outer similarity laws to give in implicit form

$$\frac{0.3462(3.889 - H)}{H} \sigma + 0.9392 A \ln \sigma = A \ln R_\theta + B_1 - 2.0938 A$$

$$- A \ln \left[(H - 1)^{0.9392}/H^{1.9392}\right] \tag{58}$$

where

$$\sigma = \left(\frac{\tau_w}{\rho U^2}\right)^{-1/2} \tag{59}$$

and B_1 is a law-of-the-wall (inner) law factor which is constant for smooth surfaces and a variable for rough surfaces and drag-reducing polymer solutions.

The variation of σ with H and R_θ required in the next section is derived in Reference 11 for smooth surfaces (B_1 = constant) as

$$\frac{1}{\sigma}\frac{\partial\sigma}{\partial H} = \frac{2.8885}{H(H-1)}\left[\frac{1.3462\,(H-1)\,\sigma + A\,H(H-1.9392)}{(3.889-H)\,\sigma + 2.7129\,A\,H}\right] \tag{60}$$

and

$$\frac{1}{\sigma}\frac{\partial\sigma}{\partial \ln R_\theta} = \frac{2.8885\,A\,H}{(3.889-H)\,\sigma + 2.7129\,A\,H} \tag{61}$$

ENTRAINMENT SHAPE PARAMETER AND ENTRAINMENT FACTOR

The similarity laws provide a two-parameter evaluation of entrainment shape parameter $\widetilde{H}$, which is derived in detail in Reference 11 as

$$\widetilde{H} = \left(\frac{H^2}{H-1}\right)\left(1.4857 + \frac{0.4739\,A}{G} + \frac{5A^2}{G^{2.75}}\right) - H \tag{62}$$

Also

$$\frac{\partial\widetilde{H}}{\partial H} = \frac{\widetilde{H}(H-2)-H}{H(H-1)} - \frac{H^2}{(H-1)}\left(\frac{0.4739\,A}{G} + \frac{13.75\,A^2}{G^{2.75}}\right)\left[\frac{1}{H(H+1)} + \frac{1}{\sigma}\frac{\partial\sigma}{\partial H}\right] \tag{63}$$

and

$$\frac{\partial\widetilde{H}}{\partial \ln R_\theta} = -\left(\frac{H^2}{H-1}\right)\left(\frac{0.4739\,A}{G} + \frac{13.75\,A^2}{G^{2.75}}\right)\left(\frac{1}{\sigma}\frac{\partial\sigma}{\partial \ln R_\theta}\right) \tag{64}$$

The entrainment factor E, derived in detail from equilibrium pressure gradients in Reference 11, is

$$E = \left\{H + \frac{\partial\widetilde{H}}{\partial \ln R_\theta} - \left(\frac{\partial\widetilde{H}}{\partial H}\right)\left[\frac{A\,H(H-1)^2}{A(H-1)^2 + G\,H}\right]\right\}\left\{\left[1 + \frac{(H+1)}{H}\beta\right]\frac{1}{\sigma^2} + \frac{\hat{p}+\hat{\sigma}}{\rho U^2}\right\} \tag{65}$$

where

$$\beta = \left(\frac{\widetilde{G} + a_3}{a_1}\right)^2 - a_2 \tag{66}$$

$$\widetilde{G} = G + \Delta G \tag{67}$$

$$\Delta G = -0.16\,\sigma + 3.92 \quad , \qquad 19.7 \leqslant \sigma \leqslant 24.5 \tag{68}$$

$$\Delta G = 0 \quad , \qquad \sigma \geqslant 24.5 \tag{69}$$

ΔG represents an effect due to low Reynolds number which is important in calculating the turbulent boundary layer just after transition from laminar flow.

QUADRATIC SHAPE PARAMETERS

From previous definitions, the quadratic displacement shape parameter H_Δ may be written in the form

$$H_\Delta = \frac{\Delta/\delta^2}{(\theta/\delta)^2} \tag{70}$$

where

$$\frac{\Delta}{\delta^2} = \int_0^1 \left(1 - \frac{u}{U}\right)\left(\frac{y}{\delta}\right) d\left(\frac{y}{\delta}\right) \tag{71}$$

and

$$\frac{\theta}{\delta} = \int_0^1 \left(1 - \frac{u}{U}\right)\left(\frac{u}{U}\right) d\left(\frac{y}{\delta}\right) \tag{72}$$

Evaluation of H_Δ depends on the choice of velocity profile $\frac{u}{U}\left[\frac{y}{\delta}\right]$. First a simple power-law velocity profile will be used as a basis of comparison. Then a two-parameter velocity profile arising from the velocity similarity laws will be utilized to derive a relation for H_Δ.

The power-law velocity profile is given by

$$\frac{u}{U} = \left(\frac{y}{\delta}\right)^n \tag{73}$$

where n is a constant.

Elementary integration in Equations (71) and (72) results in

$$H_\Delta = \frac{H^2 (H + 1)^2}{2(H - 1)(H + 3)} \tag{74}$$

where H obtained from integrations of Equations (28) and (29) is substituted for n.

From the velocity-similarity laws, H_Δ is derived as follows from the definition of J_1 in Equation (47) and from Equation (71)

$$\frac{\Delta}{\delta^2} = \frac{J_1}{\sigma} \tag{75}$$

From the definitions of I_1 in Equation (46), and H in Equation (30)

$$\frac{\theta}{\delta} = \frac{I_1}{\sigma H} \tag{76}$$

Then

$$H_\Delta = \sigma H^2 \left(\frac{J_1}{I_1^2}\right) \tag{77}$$

From the definition of G in Equation (50) and H in Equation (30)

$$\sigma = \left(\frac{H}{H-1}\right) G \tag{78}$$

Consequently

$$H_\Delta = \frac{H^3}{(H-1)} \left(\frac{G J_1}{I_1^2}\right) \tag{79}$$

$\left(\frac{G J_1}{I_1^2}\right)$ is related to G by means of Equations (50), (54), (55), and (56) with B_2 as the implicit parameter. At the limiting condition of separation $B_2 \to \infty$, and $\frac{G J_1}{I_1^2} \to \frac{78}{175}$.

A numerical fit of calculated values of $\frac{G J_1}{I_1^2}$ as a function of G gives the approximation

$$\frac{G J_1}{I_1^2} = \frac{78}{175} + \frac{3A}{G^3} \tag{80}$$

which satisfies the condition at separation where $G \to \infty$.

Then finally from Equations (79) and (78)

$$H_\Delta = \frac{78}{175} \frac{H^3}{(H-1)} + \frac{3 A H^6}{(H-1)^4} \frac{1}{\sigma^3} \tag{81}$$

The quadratic momentum shape parameter H_ϕ may be written in the form

$$H_\phi = \frac{\phi/\delta^2}{(\theta/\delta)^2} \tag{82}$$

where

$$\frac{\phi}{\delta^2} = \int_0^1 \left(1 - \frac{u}{U}\right)\left(\frac{u}{U}\right)\left(\frac{y}{\delta}\right) d\left(\frac{y}{\delta}\right) \tag{83}$$

and $\frac{\theta}{\delta}$ is given by Equation (72).

Use of the power-law velocity Equation (73) results in

$$H_\phi = \frac{H^2 (H + 1)}{(H + 3)(H - 1)} = \frac{2 H_\Delta}{H + 1} \tag{84}$$

For the velocity similarity laws H_ϕ is derived as follows. From the definition of J_1 in Equation (47) and J_2 in Equation (49)

$$\frac{\phi}{\delta^2} = \frac{J_1}{\sigma} - \frac{J_2}{\sigma^2} \tag{85}$$

Use of $\frac{\theta}{\delta}$ in Equation (76) and Equation (78) for σ results in

$$H_\phi = \frac{H^3}{(H - 1)}\left(\frac{G J_1}{I_1^2}\right) - H^2\left(\frac{J_2}{I_1^2}\right) \tag{86}$$

$\frac{G J_1}{I_1^2}$ has already been evaluated in Equation (80).

$\frac{J_2}{I_1^2}$ is related to G by means of Equation (57) and (54) with B_2 as the implicit parameter. At the limiting condition of separation $B_2 \to \infty$, and $\frac{J_2}{I_1^2} \to \frac{12}{35}$. $\frac{J_2}{I_1^2}$ as a function of G gives the approximation

$$\frac{J_2}{I_1^2} = \frac{12}{35} - \frac{0.1821\, A}{G} \tag{87}$$

which satisfies the condition at separation where $G \to \infty$. Using the relationship between σ and G in Equation (78) results in

$$H_\phi = \frac{0.1028\, H^2 (H + 3.336)}{H - 1} + \left(\frac{0.1821\, A H^3}{H - 1}\right)\frac{1}{\sigma} + \left[\frac{3 A H^6}{(H - 1)^4}\right]\frac{1}{\sigma^3} \tag{88}$$

The quadratic entrainment shape parameter is given by Equation (43) as

$$H_\psi = \frac{1}{2}\left(\frac{\delta}{\theta}\right)^2 - H_\Delta$$

For power-law velocity profiles Equation (73)

$$\frac{\delta}{\theta} = \frac{H(H+1)}{H-1} \tag{89}$$

Then from Equation (74) for H_Δ, it follows that

$$H_\psi = \frac{2H^2(H+1)^2}{(H-1)^2(H+3)} \tag{90}$$

For the velocity similarity laws

$$\frac{\delta}{\theta} = \left(\frac{H^2}{H-1}\right)\left(1.4857 - \frac{0.474\,A}{G} + \frac{5A^2}{G^{2.75}}\right) \tag{91}$$

using Equations (41) and (62).

Finally

$$H_\psi = \frac{H^4}{2(H-1)^2}\left[1.4857 - \frac{0.474\,AH}{(H-1)}\frac{1}{\sigma} + 5A^2\left(\frac{H}{H-1}\right)^{2.75}\frac{1}{\sigma^{2.75}}\right]^2 - \frac{78}{175}\frac{H^3}{(H-1)} - \frac{3AH^6}{(H-1)^4}\frac{1}{\sigma^3} \tag{92}$$

from Equations (78), (81), (43), and (91).

The quadratic shape parameters H_Δ, H_ϕ, and H_ψ are shown in Figures 2 through 4. Calculations of the similarity law formulations are based on values of the constants for the similarity laws as given in Reference 11. Here the values of the constants are given by $A = 2.606$ and $B_1 = 3.88$, which are chosen so that the drag coefficient closely fits the well-accepted Schoenherr formula for smooth flat plates for the case of zero pressure gradient. Since the similarity laws provide a two-parameter variation, the quadratic shape parameters vary with Reynolds numbers as well as H. The plots show the variation of H_Δ, H_ϕ, and H_ψ at two momentum thickness Reynolds numbers, $R_\theta = 10^3$ and 10^5. It is to be noted that the greatest effect of Reynolds number variations is at the lower values of H. For comparison the power-law relations are also plotted. The agreement at high Reynolds numbers is surprisingly close.

Experimental values obtained by Patel et al.[13,14] are also plotted. Values of H_Δ, H_ϕ, and H_ψ for a thin, axisymmetric boundary layer $\frac{\delta}{r_w} < 0.2$ are not plotted inasmuch as the

[13]Patel, V.C. et al., "An Experimental Study of the Thick Turbulent Boundary Layer Near the Tail of a Body of Revolution," Iowa Institute of Hydraulic Research Report 142 (Jan 1973).

[14]Patel, V.C., "Measurements in the Thick Axisymmetric Turbulent Boundary Layer Near the Tail of a Body of Revolution," Journal of Fluid Mechanics, Vol. 63, part 3, pp. 345-367 (1974).

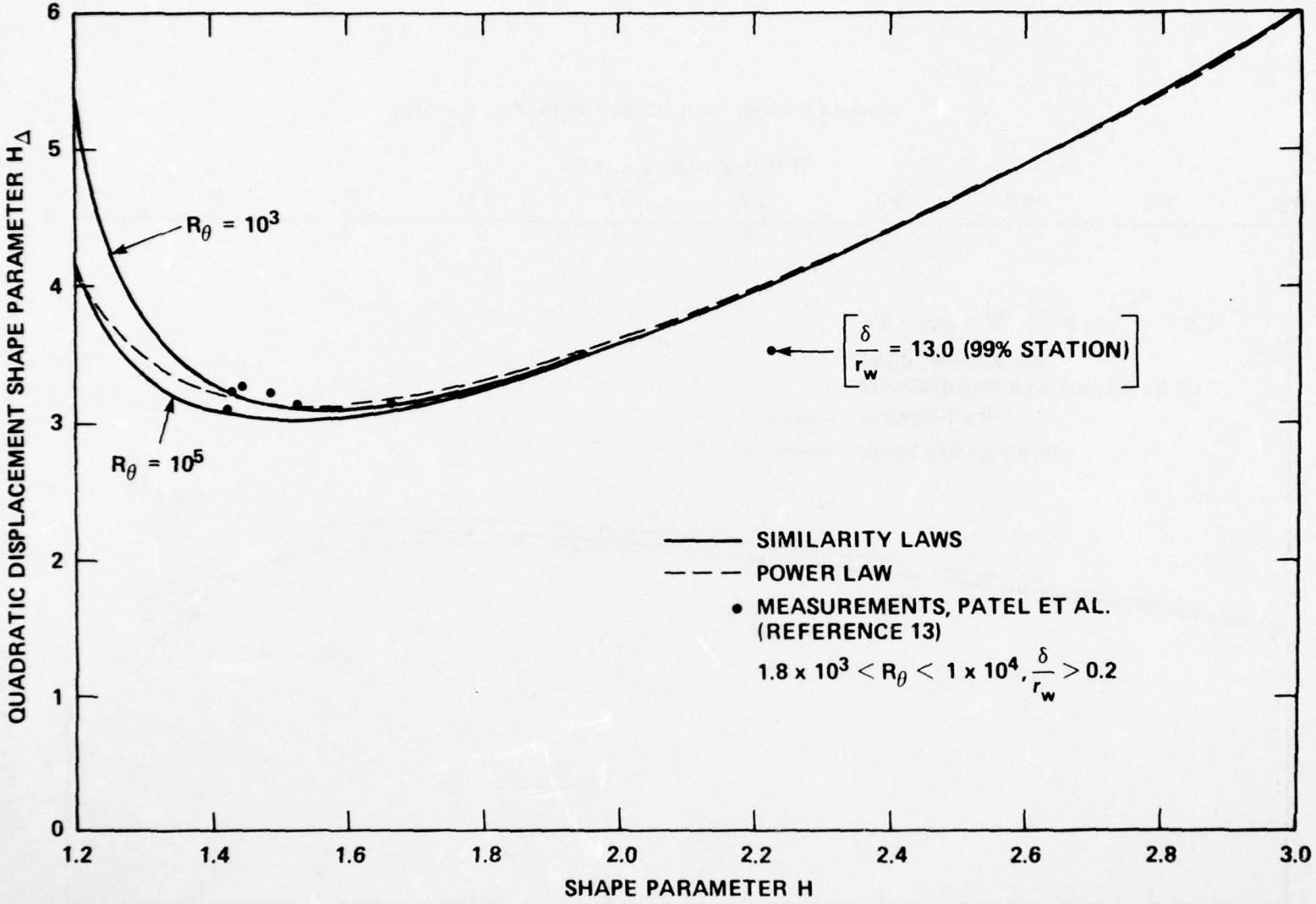

Figure 2 – Quadratic Displacement Shape Parameter

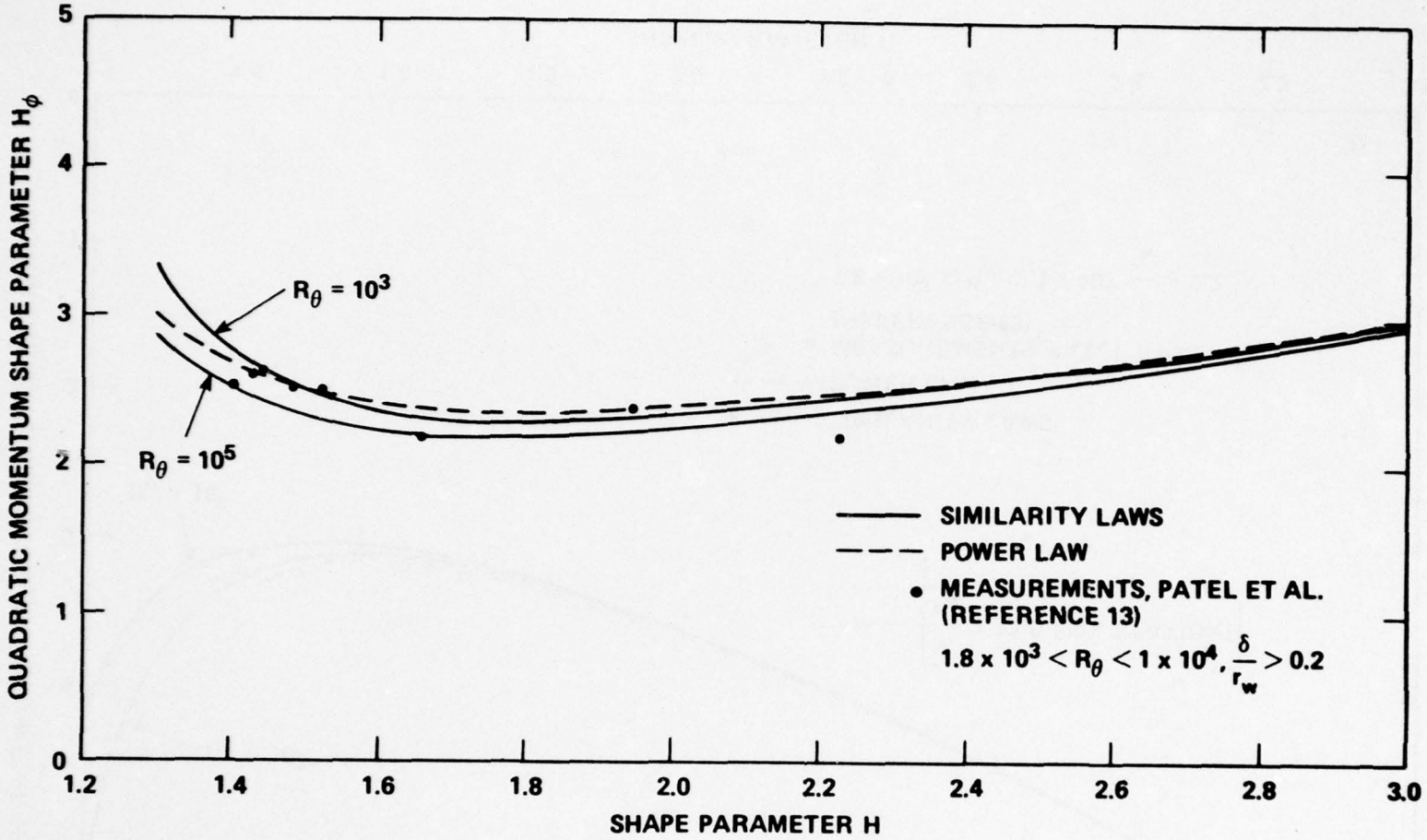

Figure 3 – Quadratic Momentum Shape Parameter

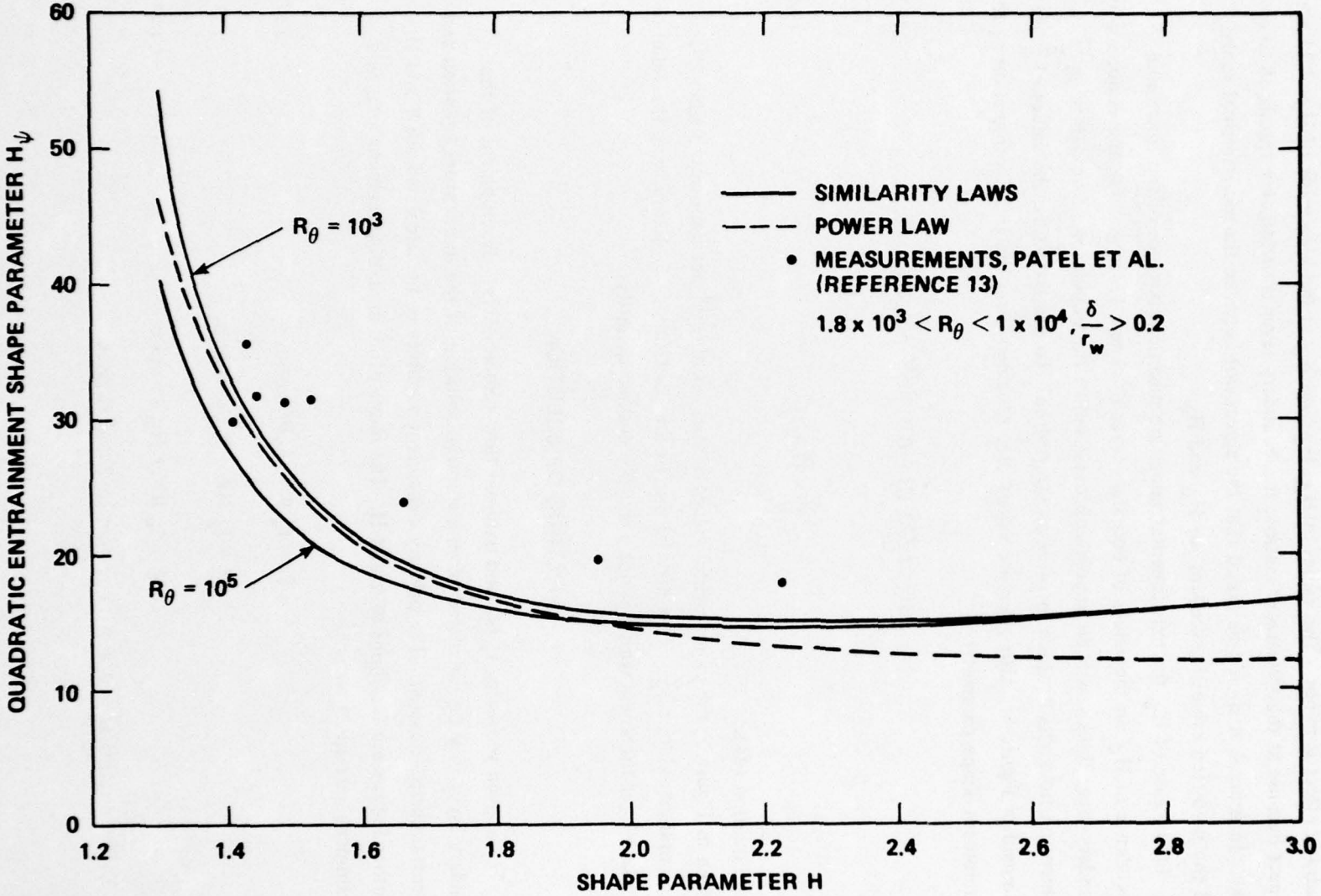

Figure 4 – Quadratic Entrainment Shape Parameter

quadratic effect is minor. The values of H_Δ, H_ϕ, and H_ψ at the high value of H = 2.23 are suspect because at the 99-percent station, the boundary layer is undergoing transition to a wake. In general, it should be noted that the agreement between the experimental values and the predicted values is excellent for H_Δ and H_ϕ.

In the case of H_ψ the experimental values are uncertain because of the functional dependence of H_ψ on the values of boundary-layer thickness δ. In general, the evaluation of boundary-layer thickness is an imprecise process unlike the evaluation of boundary-layer momentum thickness θ which involves an integration. To illustrate this, the values of $\frac{\delta}{\theta}$ are examined in Figure 5. Also given are values of $\frac{\delta}{\theta}$ obtained from the Head formulation of the entrainment shape parameter $\widetilde{H}$[11]

$$\widetilde{H} = 1.535\ (H - 0.7)^{-2.715} + 3.3 \tag{93}$$

and

$$\frac{\delta}{\theta} = \widetilde{H} + H \tag{94}$$

from Equation (41).

As seen in Figure 5, the experimental values of Patel et al.[13,14] are uniformly higher than the computed values of $\frac{\delta}{\theta}$. This may be due to the uncertainity in determining the value of boundary-layer thickness which is not a sharply defined quantity.

METHOD OF SOLUTION

For a given geometry $r_w[s]$ and external flow velocity U[s], development of the boundary layer may be calculated from a stepwise solution of the momentum equation and the entrainment equation. The primary dependent variables to be calculated are θ and H. All other factors are functions of θ and H. The momentum area, displacement area, and entrainment area are

$$\Omega = r_w \theta + H_\phi \theta^2 \cos\alpha \tag{37}$$

$$\Lambda^* = r_w H\theta + H_\Delta \theta^2 \cos\alpha \tag{38}$$

$$\psi = r_w \widetilde{H}\theta + H_\psi \theta^2 \cos\alpha \tag{40}$$

Differentiating Ω and ψ with respect to θ and H gives

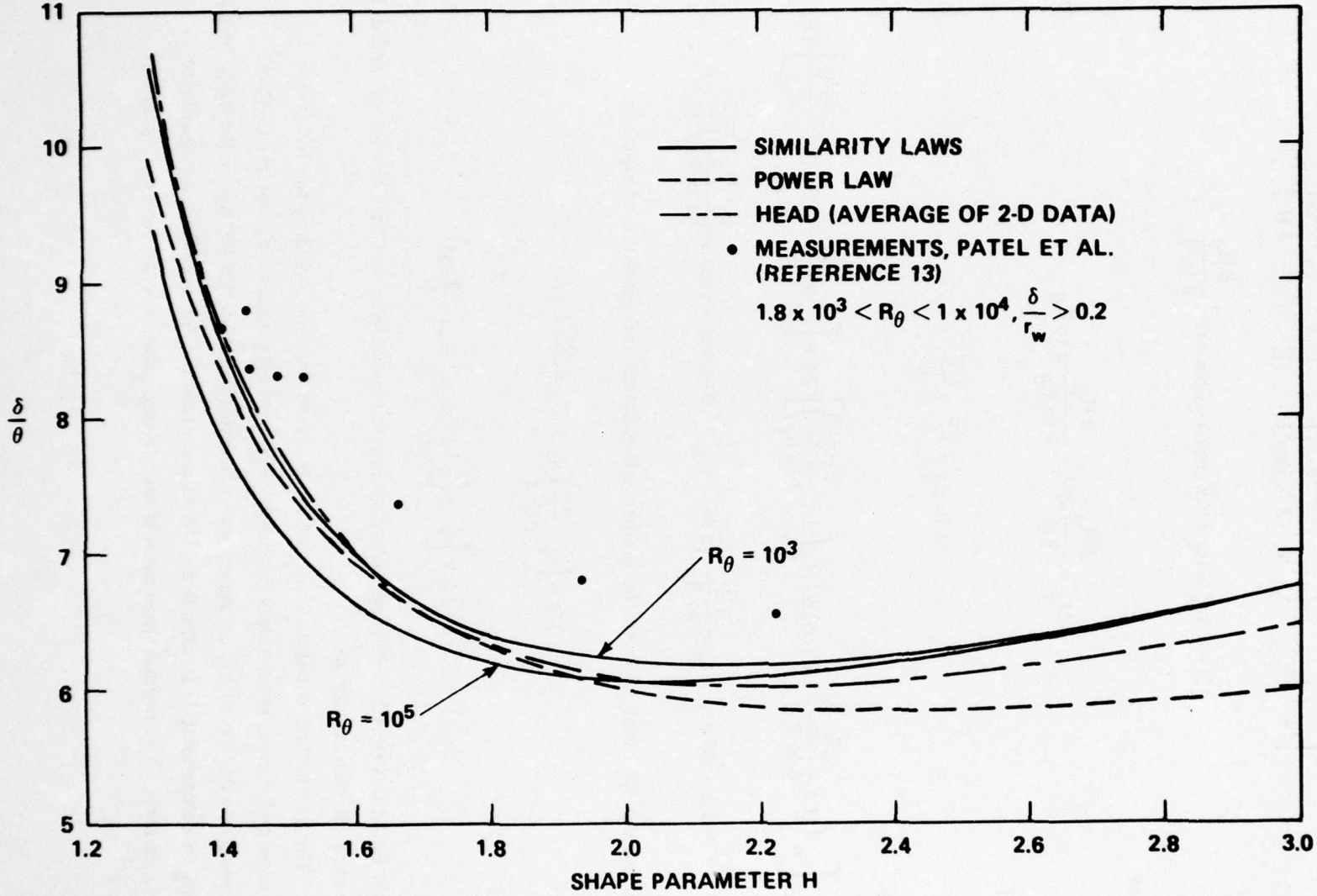

Figure 5 – Ratio of Boundary-Layer to Momentum Thicknesses

$$\left[r_w + \theta(\cos\alpha)\left(2H_\phi + \frac{\partial H_\phi}{\partial \ln R_\theta}\right)\right] d\theta + \left[(\cos\alpha)\theta^2 \frac{\partial H_\phi}{\partial H}\right] dH$$

$$= d\Omega - \theta\, dr_w - H_\phi \theta^2\, d(\cos\alpha) - (\cos\alpha)\theta^2 \frac{\partial H_\phi}{\partial \ln R_\theta} \frac{dU}{U} \tag{93}$$

since

$$dH_\phi = \frac{\partial H_\phi}{\partial H} dH + \frac{\partial H_\phi}{\partial \ln R_\theta} d\ln R_\theta \tag{94}$$

and

$$d\ln R_\theta = \frac{d\theta}{\theta} + \frac{dU}{U} \tag{95}$$

and

$$\left[r_w\left(H + \frac{\partial \tilde{H}}{\partial \ln R_\theta}\right) + \theta(\cos\alpha) H_\psi\left(2 + \frac{\partial H_\psi}{\partial \ln R_\theta}\right)\right] d\theta + \left[r_w \theta \frac{\partial \tilde{H}}{\partial H} + (\cos\alpha)\theta^2 \frac{\partial H_\psi}{\partial H}\right] dH$$

$$= d\psi - \tilde{H}\theta\, dr_w - r_w \frac{\partial \tilde{H}}{\partial \ln R_\theta} \frac{\theta}{U} dU - H_\psi \theta^2\, d(\cos\alpha) - (\cos\alpha)\left(\frac{\partial H_\psi}{\partial \ln R_\theta}\right)\frac{\theta^2}{U} dU \tag{96}$$

$d\Omega$ and $d\psi$ are obtained from the momentum equation and entrainment equation

$$d\Omega = \left(r_w \frac{\tau_w}{\rho U^2}\right) ds - \frac{(\Lambda^* + 2\Omega)}{U} dU \tag{97}$$

and

$$d\psi = \left[r_w + \left(\frac{\delta}{\theta}\right)\theta \cos\alpha\right] E\, ds - \frac{\psi}{U} dU \tag{98}$$

Then Equations (93) and (96) are solved as simultaneous algebraic equations for $d\theta$ and dH for each differential step ds.

The momentum equation Equation (5) is solved without including the transverse pressure and normal stress terms inasmuch as reliable formulations do not exist. Patel[5] recommends the use of the measured pressure distribution on the surface of the body instead of p_δ in determining U in Equation (16) as compensation for excluding the transverse pressure term. The normal stress term is usually negligible, except close to separation.

SUMMARY

A new entrainment equation is derived for thick axisymmetric boundary layers

$$\frac{d}{ds}\int_0^{\delta} u\, r\, dy = r_{\delta}\, UE \tag{22}$$

New quadratic shape parameters, H_{Δ}, H_{ϕ}, and H_{ψ} are introduced and evaluated by the velocity-similarity laws in two-parameter relationships, namely, as functions of H and R_{θ}. Agreement with test data is excellent. This tends to corroborate the assumption that velocity similarity laws apply also to thick, axisymmetric, turbulent boundary layers.

All the necessary analytical relations have been derived for a two-parameter calculation of thick, turbulent boundary layers in pressure gradients. The momentum loss, the boundary-layer thickness, and the velocity profile may be determined at each station in the downstream direction. All the pertinent relations are assembled in the appendix for numerical calculation of the thick, axisymmetric, turbulent boundary layer and the associated velocity profiles.

APPENDIX A
CALCULATION PROCEDURE

All the necessary analytical relations for calculating development of the thick, axisymmetric, turbulent boundary layer and the associated velocity profiles are now listed.

The pertinent equations have been nondimensionalized:

L = length of body

ℓ = axial distance from nose

$x = \ell/L$

GIVEN

$$\frac{U_\infty L}{\nu}, \frac{U}{U_\infty}[x], \frac{r_w}{L}[x]$$

SOLUTION

for $\frac{\theta}{L}$ and H

solve as simultaneous equations for $\delta\left(\frac{\theta}{L}\right)$ and δH where δ is a differential increment

$$\left[\frac{r_w}{L} + \left(\frac{\theta}{L}\right)\cos\alpha\left(2H_\phi + \frac{\partial H_\phi}{\partial \ln R_\theta}\right)\right]\delta\left(\frac{\theta}{L}\right) + \left[\left(\frac{\theta}{L}\right)^2 \cos\alpha \frac{\partial H_\phi}{\partial H}\right]\delta H$$

$$= \delta\left(\frac{\Omega}{L^2}\right) - \left(\frac{\theta}{L}\right)\delta\left(\frac{r_w}{L}\right) - H_\phi\left(\frac{\theta}{L}\right)^2 \delta(\cos\alpha) - \left(\frac{\theta}{L}\right)^2 (\cos\alpha)\frac{\partial H_\phi}{\partial \ln R_\theta}\left(\frac{U}{U_\infty}\right)^{-1}\delta\left(\frac{U}{U_\infty}\right) \quad (93)$$

$$\left[\left(\frac{r_w}{L}\right)\left(\tilde{H} + \frac{\partial \tilde{H}}{\partial \ln R_\theta}\right) + \left(\frac{\theta}{L}\right)\cos\alpha\, H_\psi\left(2 + \frac{\partial H_\psi}{\partial \ln R_\theta}\right)\right]\delta\left(\frac{\theta}{L}\right) + \left[\left(\frac{r_w}{L}\right)\left(\frac{\theta}{L}\right)\frac{\partial \tilde{H}}{\partial H}\right.$$

$$\left. + \left(\frac{\theta}{L}\right)^2 \cos\alpha \frac{\partial H_\psi}{\partial H}\right]\delta H = \delta\left(\frac{\psi}{L^2}\right) - \tilde{H}\left(\frac{\theta}{L}\right)\delta\left(\frac{r_w}{L}\right) - H_\psi\left(\frac{\theta}{L}\right)^2 \delta(\cos\alpha)$$

$$-\left[\frac{r_w}{L}\frac{\partial \tilde{H}}{\partial \ln R_\theta}\left(\frac{\theta}{L}\right)\left(\frac{U}{U_\infty}\right)^{-1} + \left(\frac{\theta}{L}\right)^2 \frac{\partial H_\psi}{\partial \ln R_\theta}\cos\alpha\left(\frac{U}{U_\infty}\right)^{-1}\right]\delta\left(\frac{U}{U_\infty}\right) \quad (96)$$

$$\cos\alpha = \left[1 + \frac{d\left(\frac{r_w}{L}\right)}{dx}\right]^{-1/2}$$

$$\delta\left(\frac{\Omega}{L^2}\right) = \frac{d(\Omega/L^2)}{dx}\,\delta x, \text{ etc.}$$

$$\frac{d(\Omega/L^2)}{dx} = \left(\frac{r_w}{L}\right)\frac{\sec\alpha}{\sigma^2} - \left(\frac{\Lambda^*}{L^2} + 2\,\frac{\Omega}{L^2}\right)\left(\frac{U}{U_\infty}\right)^{-1}\frac{d(U/U_\infty)}{dx} \tag{97}$$

$$\frac{d(\psi/L^2)}{dx} = \left[\frac{r_w}{L}\sec\alpha + \left(\frac{\delta}{\theta}\right)\left(\frac{\theta}{L}\right)\right]E - \left(\frac{\psi}{L^2}\right)\left(\frac{U}{U_\infty}\right)^{-1}\frac{d(U/U_\infty)}{dx} \tag{98}$$

$$\frac{\delta}{\theta} = \tilde{H} + H \tag{41}$$

$$H_\psi = \frac{1}{2}(\tilde{H} + H)^2 - H_\Delta \tag{43}$$

$$\frac{\partial H_\psi}{\partial \ln R_\theta} = (\tilde{H} + H)\frac{\partial \tilde{H}}{\partial \ln R_\theta} - \frac{\partial H_\Delta}{\partial \ln R_\theta}$$

$$R_\theta = \left(\frac{U}{U_\infty}\right)\left(\frac{\theta}{L}\right)\left(\frac{U_\infty L}{\nu}\right)$$

$$\frac{0.3462\,(3.889 - H)}{H}\,\sigma + 0.9392\,A\ln\sigma = A\ln R_\theta + B_1$$

$$- 2.0938\,A - A\ln\left[(H-1)^{0.9392}/H^{1.9392}\right] \tag{58}$$

$$\frac{\Lambda^*}{L^2} = \left(\frac{r_w}{L}\right)\left(\frac{\theta}{L}\right)H + H_\Delta\left(\frac{\theta}{L}\right)^2\cos\alpha \tag{37}$$

$$\frac{\Omega}{L^2} = \left(\frac{r_w}{L}\right)\left(\frac{\theta}{L}\right) + H_\phi\left(\frac{\theta}{L}\right)^2\cos\alpha \tag{38}$$

$$\frac{\psi}{L^2} = \left(\frac{r_w}{L}\right)\left(\frac{\theta}{L}\right)\tilde{H} + H_\psi\left(\frac{\theta}{L}\right)^2\cos\alpha \tag{40}$$

$$G = \sigma\left(\frac{H-1}{H}\right) \tag{50}$$

$$\tilde{H} = \left(\frac{H^2}{H-1}\right)\left(1.4857 + \frac{0.4739\,A}{G} + \frac{5\,A^2}{G^{2.75}}\right) - H \tag{62}$$

$$\frac{\partial \tilde{H}}{\partial H} = \frac{\tilde{H}(H-2) - H}{H(H-1)} - \frac{H^2}{H-1}\left(\frac{0.4739\,A}{G} + \frac{13.75\,A^2}{G^{2.75}}\right)\left[\frac{1}{H(H+1)} + \frac{1}{\sigma}\frac{\partial \sigma}{\partial H}\right] \tag{63}$$

$$\frac{\partial \tilde{H}}{\partial \ln R_\theta} = -\left(\frac{H^2}{H-1}\right)\left(\frac{0.4739\,A}{G} + \frac{13.75\,A^2}{G^{2.75}}\right)\left(\frac{1}{\sigma}\frac{\partial \sigma}{\partial \ln R_\theta}\right) \tag{64}$$

$$\frac{1}{\sigma}\frac{\partial \sigma}{\partial H} = \frac{2.8885}{H(H-1)}\left[\frac{1.3462(H-1)\sigma + A\,H(H-1.9392)}{(3.889-H)\sigma + 2.7129\,A\,H}\right] \tag{60}$$

$$\frac{1}{\sigma}\frac{\partial \sigma}{\partial \ln R_\theta} = \frac{2.8885\,A\,H}{(3.889-H)\sigma + 2.7129\,A\,H} \tag{61}$$

$$E = \left\{\tilde{H} + \frac{\partial \tilde{H}}{\partial \ln R_\theta} - \left(\frac{\partial \tilde{H}}{\partial H}\right)\left[\frac{A\,H(H-1)^2}{A(H-1)^2 + G\,H}\right]\right\}\left[1 + \frac{(H+1)}{H}\,B\right]\frac{1}{\sigma^2} \tag{65}$$

($\hat{p}$ and $\hat{\sigma}$ are assumed zero)

$$\beta = \left(\frac{\tilde{G} + a_3}{a_1}\right)^2 - a_2 \tag{66}$$

$$\tilde{G} = G + \Delta G \tag{67}$$

$$\Delta G = -0.16\sigma + 3.92 \quad , 19.7 \leqslant \sigma < 24.5 \tag{68}$$

$$\Delta G = 0 \quad , \sigma \geqslant 24.5 \tag{69}$$

$$H_\Delta = \frac{78}{175}\,\frac{H^3}{(H-1)} + \frac{3\,A\,H^6}{(H-1)^4}\,\frac{1}{\sigma^3} \tag{81}$$

$$H_\phi = \frac{0.1028\,H^2(H+3.336)}{H-1} + \left(\frac{0.1821\,A\,H^3}{H-1}\right)\frac{1}{\sigma} + \left[\frac{3\,A\,H^6}{(H-1)^4}\right]\frac{1}{\sigma^3} \tag{88}$$

$$\frac{\partial H_\Delta}{\partial H} = \frac{78}{175}\,\frac{H^2(2H-3)}{(H-1)^2} + \frac{6\,A\,H^5(H-3)}{(H-1)^5}\,\frac{1}{\sigma^3} - \frac{9\,A\,H^6}{(H-1)^4\,\sigma^3}\left(\frac{1}{\sigma}\frac{\partial \sigma}{\partial H}\right)$$

$$\frac{\partial H_\Delta}{\partial \ln R_\theta} = -\frac{9\,A\,H^6}{(H-1)^4\,\sigma^3}\left(\frac{1}{\sigma}\frac{\partial \sigma}{\partial \ln R_\theta}\right)$$

$$\frac{\partial H_\phi}{\partial H} = \frac{0.2056\,H(H^2 + 0.168\,H - 3.336)}{(H-1)^2} - \frac{A\,H^3}{(H-1)}\left[\frac{0.1821}{\sigma} + \frac{9H^3}{(H-1)^3\,\sigma^3}\right]\left(\frac{1}{\sigma}\,\frac{\partial \sigma}{\partial H}\right)$$

$$+ \frac{0.1821\,A\,H^2(2H-3)}{(H-1)^2\,\sigma} + \frac{6A\,H^5(H-3)}{(H-1)^5\,\sigma^3}$$

$$\frac{\partial H_\phi}{\partial \ln R_\theta} = -\frac{A\,H^3}{(H-1)}\left[\frac{0.1821}{\sigma} + \frac{9H^3}{(H-1)^3\,\sigma^3}\right]\left(\frac{1}{\sigma}\,\frac{\partial \sigma}{\partial \ln R_\theta}\right)$$

$$A = 2.606$$

$$B_1 = 3.88$$

$$a_1 = 6.1,\ a_2 = 1.81,\ a_3 = 1.37$$

INITIAL CONDITIONS AT TRANSITION (Reference 11)

$$(R_\theta)_{turb} = (R_\theta)_{lam} + \Delta R_\theta$$

$$\frac{1}{H_o} = 1 - \frac{\tilde{G}_o + \Delta G[\sigma_o]}{\sigma_o}$$

$$\tilde{G}_o = 6.84$$

$$\Delta G = 0.16\,\sigma_o + 3.92$$

$$\sigma_o = 3.22 \ln R_\theta - 1.46$$

VELOCITY PROFILE (Reference 11)

$$I_1 = \frac{G}{1.4857 + \dfrac{0.4739\,A}{G} + \dfrac{5A^2}{G^{2.75}}}$$

$$B_2 = 2\,I_1 - \frac{11}{6}\,A \qquad (54)$$

$$u_\tau = \frac{U}{\sigma}$$

$$\frac{u_\tau \delta}{\nu} = e^{\frac{\sigma - B_1 - B_2}{A}}$$

$$\delta = \frac{\nu}{u_\tau}\left(\frac{u_\tau \delta}{\nu}\right)$$

Velocity profile for $\left(\frac{u_\tau y}{L}\right)_L \leq \frac{u_\tau y}{\nu} \leq \frac{u_\tau \delta}{\nu}$

$$\frac{u}{u_\tau} = A \ln\left(\frac{u_\tau y}{\nu} - J\right) + B_1 + B_2 \frac{w}{2} + Aq$$

$$\frac{w}{2} = 3\left(\frac{y}{\delta}\right)^2 - 2\left(\frac{y}{\delta}\right)^3$$

$$q = \left(\frac{y}{\delta}\right)^2 \left(1 - \frac{y}{\delta}\right)$$

$$J = B_1 + A \ln A - A$$

$$\left(\frac{u_\tau y}{\nu}\right)_L = B_1 + A \ln A$$

Velocity profile for $0 \leq \frac{u_\tau y}{\nu} \leq \left(\frac{u_\tau y}{\nu}\right)_L$

laminar sublayer $\frac{u}{u_\tau} = \frac{u_\tau y}{\nu}$.

REFERENCES

1. Nelson, D.M., "A Turbulent Boundary-Layer Calculation Method, Based on the Law of the Wall and the Law of the Wake," U.S. Naval Ordnance Test Station (China Lake, Calif.), NavWeps Report 8510 (NOTS TP 3493) (Nov 1964).

2. Nelson, D.M., "Turbulent Boundary-Layer Calculations, Using a Law of the Wall-Law of the Wake Method," U.S. Naval Ordnance Test Station (China Lake, Calif.), NOTS TP 4083 (Jun 1966).

3. Cebeci, T. and A.M.O. Smith, "A Finite-Difference Method for Calculating Compressible Laminar and Turbulent Boundary Layers," Journal of Basic Engineering, Transactions of the American Society of Mechanical Engineers, Vol. 92, Series D, No. 3, pp. 523-535 (Sep 1970).

4. Patel, V.C., "On the Equations of a Thick Axisymmetric Turbulent Boundary Layer," Iowa Institute of Hydraulic Research Report 143 (Jan 1973).

5. Patel, V.C., "A Simple Integral Method for the Calculation of Thick Axisymmetric Turbulent Boundary Layers," Aeronautical Quarterly, Vol. 25, part 1, pp. 47-58 (Feb 1974).

6. Günther, W., "Ein mehrparametrisches Rechenfahren für turbulente, inkompressible Grenzschichten an umströmten Rotationskörpern," Fortschritt-Berichte der VDI Zeitschriften, Series 7, No. 34 (Oct 1973).

7. White, F.M. et al., "Analysis of Turbulent Skin Friction in Thick Axisymmetric Boundary Layers," American Institute of Aeronautics and Astronautics Journal, Vol. 11, No. 6, pp. 821-835 (Jun 1973).

8. Granville, P.S., "The Calculation of the Viscous Drag of Bodies of Revolution," David Taylor Model Basin Report 849 (Jul 1953).

9. Head, M.R., "Entrainment in the Turbulent Boundary Layer," Aeronautical Research Council (British), R&M 3152 (Sep 1958).

10. Shanebrook, J.R. and W.J. Sumner, "Entrainment Theory for Axisymmetric Turbulent, Incompressible Boundary Layers," Journal of Hydronautics, Vol. 4, No. 4, pp. 159-160 (Oct 1970).

11. Granville, P.S., "Similarity-Law Entrainment Method for Turbulent Boundary Layers in Pressure Gradients," DTNSRDC Report 4657 (Dec 1975).

12. Granville, P.S., "A Modified Velocity Similarity Law for Turbulent Shear Flows," NSRDC Report 4639 (May 1975).

13. Patel, V.C. et al., "An Experimental Study of the Thick Turbulent Boundary Layer Near the Tail of a Body of Revolution," Iowa Institute of Hydraulic Research Report 142 (Jan 1973).

14. Patel, V.C., "Measurements in the Thick Axisymmetric Turbulent Boundary Layer Near the Tail of a Body of Revolution," Journal of Fluid Mechanics, Vol. 63, part 3, pp. 345-367 (1974).

INITIAL DISTRIBUTION

Copies	
1	U.S. ARMY TRANS R&D Marine Trans Div
1	DOD, ARPA
4	CHONR 3 Code 438 1 Code 460
2	NRL 1 R.J. Hansen
2	USNA 1 Bruce Johnson 1 Library
3	NAVPGSCOL 1 T. Sarpkaya
1	NROTC & NAVADMINU, MIT
1	NAVWARCOL
1	NELC
6	NAVUSEACEN San Diego 1 A.G. Fabula 1 T. Lang 1 J.W. Hoyt 1 G.L. Donahue 1 D.M. Nelson
1	NAVWPNSCEN
3	NSWC White Oak 1 V.C. Dawson 1 J.E. Goeller
5	NUSC NPT 1 P. Gibson 1 J.F. Brady 1 R.H. Nadolink
1	NLONLAB NUSC
9	NAVSEASYSCOM 2 SEA 09G32 1 SEA 03C 1 SEA 03 2 SEA 033 1 SEA 035A 2 PMS-395

Copies	
2	NAVAIRSYSCOM
4	NAVSEC 1 SEC 6110.01 1 SEC 6114 1 SEC 6114D 1 SEC 6115
2	AFSOR
12	DDC
3	Bureau of Standards Mechanics Div 1 P.S. Klebanoff 1 G. Kulin
1	MARAD Div of Ships R&D
2	NASA HQS 1 A. Gessow
1	National Science Foundation Eng Sci Div
1	Univ of Bridgeport E.M. Uram, Dept Mech Eng
2	Univ of Calif Berkeley Dept of NA
3	Calif Inst of Technol 1 A.J. Acosta 1 Sabersky 1 D. Coles
3	Catholic Univ Dept of Mech Eng 1 M.J. Casarella 1 P.K. Chang
2	Davidson Lab, Stevens Inst of Tech
3	State Univ of Iowa Inst of Hydraulic Res 1 L. Landweber 1 V.C. Patel

Copies	
4	Mass Inst of Technol Dept of Ocean Eng 1 Library 1 J.N. Newman 1 P. Mandel 1 M. Abkowitz
2	Univ of Michigan Dept of NAME
3	Univ of Minnesota St. Anthony Falls Hydr Lab 1 R. Arndt
4	Penn State Univ Advanced Research Lab 1 J.L. Lumley 1 R.E. Henderson 1 B.R. Parkin
2	Univ of Rhode Island 1 F.M. White, Dept Mech Eng 1 T. Kowalski, Dept Ocean Eng
2	Stanford Univ 1 E.Y. Hsu, Dept Civil Eng 1 S.J. Kline, Dept Mech Eng
1	VPI
2	Worcester Polytech Inst Alden Res Labs 1 L.C. Neale
1	SNAME
2	Boeing Aircraft, Seattle, Wash.
1	Douglas Aircraft, Long Beach, Calif 1 T. Cebeci
1	Exxon Math & Systems, Inc R. Bernicker
3	Hydronautics, Inc 1 M.P. Tulin 1 R. Barr
1	LTV Adv Tech Center C.S. Wells, Jr.
1	Oceanics, Inc A. Lehman

Copies	
3	Rand Corp 1 E.R. van Driest 1 J. Aroesty 1 C. Gazley
1	Westinghouse Electric M.S. Macovsky

CENTER DISTRIBUTION

Copies	Code	
1	1500	
1	1504	
1	1520	
1	1540	
100	1541	P.S. Granville
3	1552	J.H. McCarthy
1	1556	
1	1560	
1	1802.2	
1	1802.3	
1	1802.4	
1	1843	
1	1900	
1	1940	
1	1942	
30	5214.1	Reports Distribution
1	5221	Library (C)
1	5222	Library (A)

QUADRATIC MOMENTUM SHAPE PARAMETER H_4